Femtosecond Laser Processing System with Target Tracking Feature

Akihiro TAKITA, Yoshio HAYASAKI and Nobuo NISHIDA

Department of Optical Science and Technology, Faculty of Engineering,
The University of Tokushima,
2-1 Minamijosan jima-cho, Tokushima 770-8506, Japan
E-mail: takita@opt.tokushima-u.ac.jp

A femtosecond laser processing system with a target tracking feature was developed. The block matching method based on a sum-of-squared-difference metric was used to measure the transverse movement of a target. Surface position was detected with an astigmatic sensor to measure the axial movement. The maximum tracking speeds of the target in the transverse and axial directions were 150 and 100 µm/s, respectively. A square traveling sample and an inclined sample were processed.

Keywords: femtosecond laser processing, biological tissue, focus control

1. Introduction

Femtosecond laser processing has several advantages, including the ability to process inside transparent materials three-dimensionally, a spatial resolution smaller than the diffraction limit, and little thermal damage [1]. Femtosecond laser processing has been applied to fabricate three-dimensional microstructures in glasses, polymers, and biological tissues [2-4]. Our group has investigated the use of biological tissue processed with a femtosecond laser for optical memory [5-7]. An array of bits is recorded by irradiating a human fingernail with femtosecond laser pulses, and the bits are subsequently read by observing fluorescence produced inside the fingernail in vitro. Biological tissue, however, typically exhibits motion in vivo and typically has complex curved and bumpy surfaces. Therefore, a femtosecond laser processing system for biological tissue must detect the movement of a target and adjust the focus during processing.

In this paper, we describe a femtosecond laser processing system with a target tracking feature developed in our laboratory. A complementary metal oxide semiconductor (CMOS) image sensor and a guide laser were used to measure the movement of a target in the transverse and axial directions. A piezoelectric transducer (PZT) was used to adjust the focus in response to the detected surface movement.

2. Experimental procedure

2.1 Experimental setup

Figure 1 shows our femtosecond laser processing system with a target tracking feature. The system was composed of a femtosecond laser processing system, a He-Ne laser, a metal-halide light source, a CMOS image sensor, an objective lens (×40, 0.55 NA) with a three-axis PZT actuator, and a three-axis motorized stage. The femtosecond laser system generated pulses with a center wavelength of 800 nm, a pulse duration of 150 fs, and a repetition rate of 1 to 1000 Hz. The CMOS image sensor acquired a surface reflection image of a processing target and an ellipse of the He-Ne laser spot, which was formed astigmatically by a pair of cylindrical lenses. Movement of the sample in the transverse direction was measured by using a block matching method using the reflection image, and movement in the axial direction was measured by detecting the surface position with an astigmatic sensor. The focus of the objective was adjusted with the PZT actuator to follow the measured movement. Irradiation of femtosecond laser pulses was controlled with a shutter. The CMOS image sensor, the shutter, the three-axis PZT stage, and the three-axis motorized stage were controlled by a computer.

2.2 Block matching method using sum of squared difference metric

The block matching method was used to measure movement of the target in the transverse direction [8, 9]. In this method, the similarity between a clipped area of the current frame and a pre-acquired image of the tracking target was calculated. The sum of squared difference (SSD) metric was used to compute the similarity. The SSD is defined as:

$$R_{SSD}(x, y) = \sum_{u,v}^{W} \left[I_1(x+u, y+v) - I_2(u,v)\right]^2, \qquad (1)$$
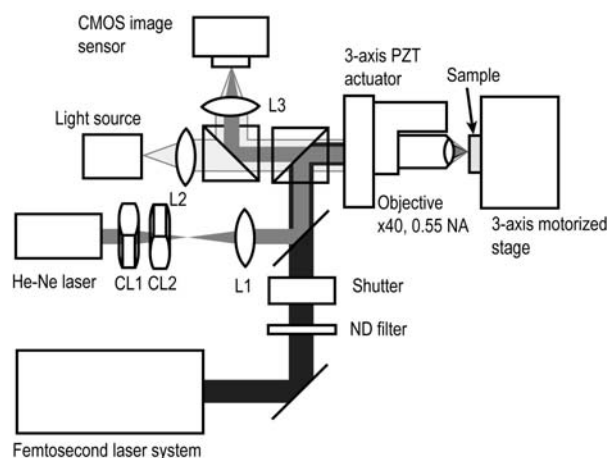

Fig. 1 Experimental setup. L1: lens (f = 200 mm), L2: lens (f = 50 mm), L3: lens (f = 300 mm), CL1: cylindrical lens (f = 200 mm), and CL2: cylindrical lens (f = 150 mm).

where (x, y) is the top-left position of the clipped area on the captured image, $I_1(u, v)$ and $I_2(u, v)$ are intensities at positions (u, v) in the clipped image and a tracking target image, and W is the size of the clipped area. Coordinates of the minimum R_{SSD} give the position where the tracking target is in the current frame. The difference of the coordinates between the previous frame and the current frame is the movement of the processing target during one frame.

To find the coordinates of the minimum R_{SSD}, two different methods can be used. One method is the exhaustive search method. In this method, R_{SSD} is computed in the entire area of the current image to find the minimum R_{SSD}. In this method, R_{SSD} must be computed $N = (W_c - W_t) \times (H_c - H_t)$ times, where W_c and H_c are the width and height of the captured image, and W_t and H_t are the width and height of the target image. Therefore, an exhaustive search needs a long time when the image size becomes large.

The other method is to use the steepest descent method. In this method, first, the area-of-interest (AOI) is set to center of the captured image and R_{SSD} there is computed. Second, the four R_{SSD} values of the neighboring coordinates around the AOI are calculated. If the R_{SSD} of a neighboring point is smaller than R_{SSD} of the AOI, the AOI is moved to the point where R_{SSD} is smallest, and this process is repeated. If R_{SSD} of the current AOI is smaller than those of the neighboring areas, the algorithm is stopped and the coordinates of the AOI represent the coordinates of the local minimum of R_{SSD}. The coordinates of the local minimum are usually equal to the coordinates of the global minimum, but sometimes not. This algorithm needs much fewer computations of R_{SSD} than the exhaustive search method. The most appropriate method is selected to suit the kind of processing target.

Figure 2 shows the relation between the target position and measured position by computing with the exhaustive search method and the steepest descent method. The size of the captured image was 128×128 pixels, and the size of the target image was 96×96 pixels. The difference is the movement of the target position traveled from the initial position by moving the objective with the PZT actuator. The exhaustive search method was more stable than the
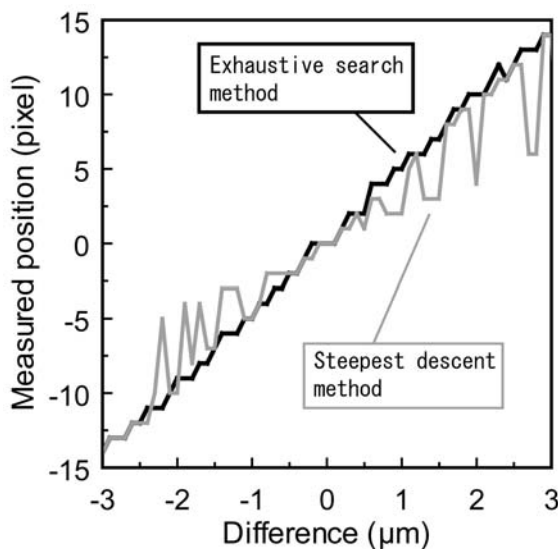
steepest descent method, because exhaustive search computes the actual minimum R_{SSD} coordinates, unlike the other method. The number of computational cycles per second was 38 in the exhaustive search method and 130 in the steepest descent method. Therefore, when a quick response is required, the steepest descent method should be selected.

2.3 Astigmatic focus error detection method

The surface movement in the axial direction was measured by the astigmatic sensor, which is of the type used in the auto-focus systems of optical disc players [10]. A He-Ne laser, a lens (L1), and two cylindrical lenses (CL1 and CL2) were arranged to produce an astigmatic difference of about 5 µm at the objective side. The resulting ellipsoidal beam spot was acquired with the CMOS camera. The astigmatic focus error was obtained by the intensity ratio of I_H to I_V, where I_H is the sum of the intensities of 8×64 pixels arranged horizontally, and I_V is the sum of the intensities of 64×8 pixels arranged vertically, as shown in Fig. 3. The intensity ratio of I_H to I_V gives the surface position.

Figure 4 shows the relations between the intensity ratio and a difference distance, namely, the distance between the objective focus and the surface position. The negative value means that the focus was below the surface. When
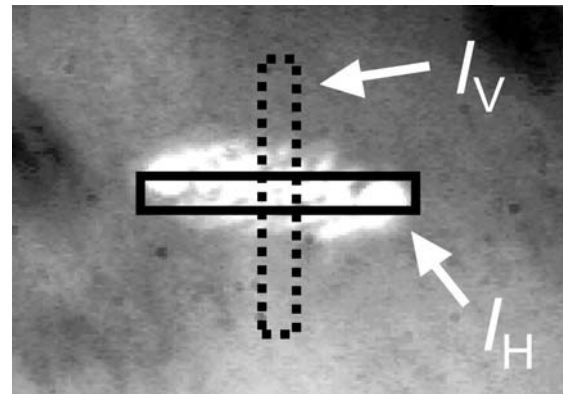

Fig. 3 Ellipsoid beam spot image. The solid rectangle shows an area for I_H, and the dotted rectangle shows an area for I_V.
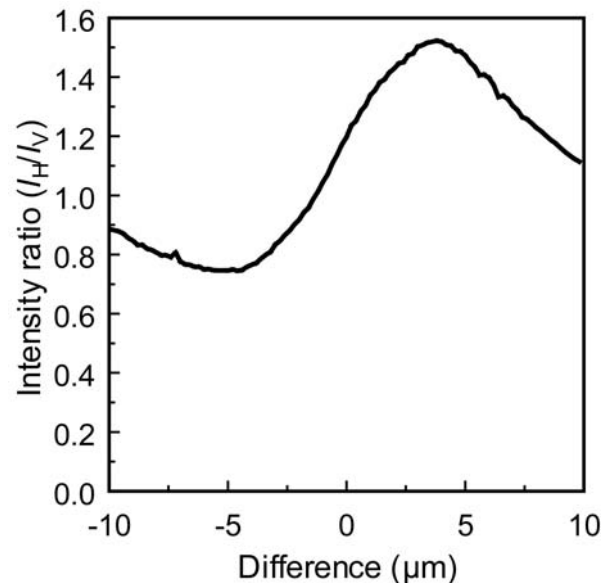

Fig. 2 Stability of movement detection. One pixel corresponds to 0.2 µm.

Fig. 4 Intensity ration vs. surface position (difference).

the intensity ratio was the minimum value, the difference was -5.4 µm. When the intensity ratio was the maximum value, the difference was 3.8 µm. Therefore, this system could measure a difference from -5.4 µm to 3.8 µm per cycle in this configuration. The detection rate of the surface position was equal to the frame rate of the CMOS image sensor. The frame rate of the CMOS image sensor was variable, depending on the captured image size (typically from 30 Hz to 130 Hz).

3. Experimental results

The processing performed with our femtosecond laser processing with target tracking was divided into processing in the transverse direction and the axial direction.

Multi-pulse drilling was performed on a traveling target. The sample was a roughly polished metal plate which was moved in the focal plane by the motorized stage. Figure 5(a) shows tracks of the focus of the femtosecond laser pulses. The area over which the target traveled was a 40-µm square and the traveling velocity was 150 µm/s. The repetition rate of the femtosecond laser pulses was 50 Hz. A pit was processed by irradiating a single femtosecond laser pulse, and multiple pits were formed in a square. Figure 5(b) shows a pit processed on the same traveling target with target tracking. The tracking target was a pit formed by irradiating ten pulses. The size of the captured image was 96 × 96 pixels. The size of target image was 48 × 48 pixels. The algorithm used was the steepest descent method, and the computational rate was about 130 Hz. The exposure time of the CMOS image sensor was 3 ms. With tracking, the processed area was smaller than the tracks shown in Fig. 5(a) because the movement of the sample was cancelled out by moving the objective lens with the PZT actuator.

The processed area in Fig. 5(b) was composed of three regions. A large ellipsoidal pit was formed at the center, and two smaller ellipsoidal pits were formed on either side of the central pit. These shapes result from the uniform motion. When the target was traveling with uniform motion, there was a fixed gap between the tracked position and the real position due to the time lag involved with capturing images, computing the minimum R_{SSD} position, and moving the objective lens. Therefore, femtosecond laser pulses were irradiated at the same difference position. The distance between the center of the central pit and the center of the left side pit was about 3.2 µm. This distance was limited by the velocity of the sample movement and the cycle time of the PZT movement. The PZT actuator required 10 ms for a movement on the order of a few micrometers. Additionally, the movement command sent to the PZT controller was actually the data for the previous cycle. Therefore, 20 ms was spent from detecting the difference to finishing moving the objective lens. This 20-ms period corresponds to 3-µm movement of the target, which travels with uniform motion at a velocity of 150 µm/s. The maximum tracking speed of the target in the transverse direction was 150 µm/s.

A pit processed on a fixed (non-tracked) sample is shown in Fig. 5(c) for comparison with Fig. 5(b). This pit was formed with the same number of the femtosecond pulses as that in Fig. 5(b). The diameter of the pit was about 4 µm. The diameter of the entire processed area, in-

cluding the three regions in Fig. 5(b), was about 10 µm. This value is near the sum of the pit diameter (4 µm) and the distances to both side pits (3.2 µm + 3.2 µm).

The surface tracking performance was measured in a simple way. Specifically, the metal sample on the motorized stage was raised and lowered by 80 µm with the stage. The maximum tracking speed of the target in the transverse direction was 100 µm/s. Figure 6 shows the precision of surface-position detection when the difference was 1.5 µm. The difference between the maximum and the minimum intensity ratio was 0.015, which corresponds to 210 nm in axial length.
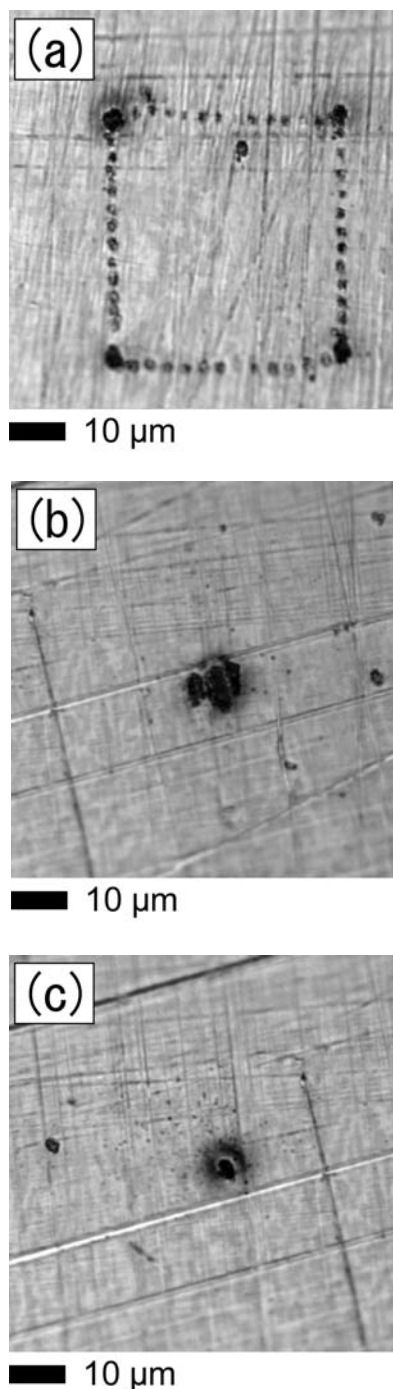

Fig. 5 Reflection images of processed structures. (a) The processing of a traveling sample without target tracking and (b) with target tracking. (c) Processing of a fixed sample, shown for comparison.
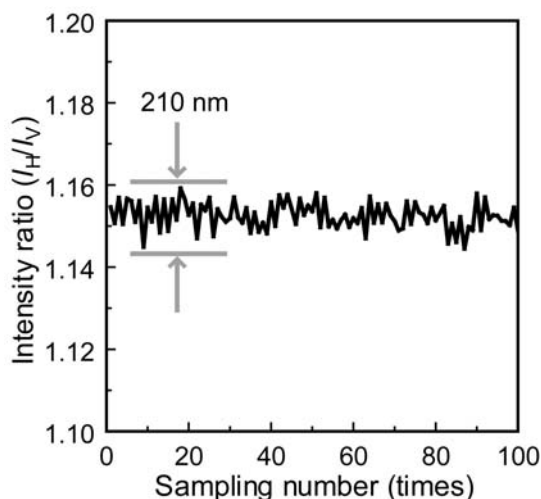
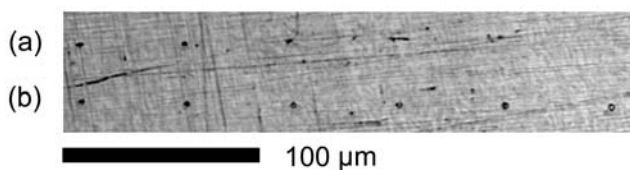**Fig. 6** Precision of surface tracking.

Fig. 7 Linearly arranged pits processed on inclined surface. The processing was performed (a) without tracking and (b) with tracking.

Figure 7 shows reflection images of lines of pits processed on a sloped surface. Figure 7(a) shows the case with surface tracking disabled, and Fig. 7(b) shows the case with surface tracking enabled. The metal sample was fixed with its surface inclined. The sample traveled by 500 µm in the transverse direction at 500 µm/s. The 500-µm travel in the transverse direction became a 30-µm travel in the axial direction, when the slope angle was 3.4°. The repetition rate of the femtosecond laser pulses was 10 Hz. When the surface tracking was disabled, the pit diameters becomes smaller, according to the traveling distance. When traveling distance was over 200 µm, the surface was too far from the focus to be formed pit. When the surface tracking was enabled, however, the focus remained on the surface. Therefore, a line of pits with the same diameter was processed.

4. Conclusion

We have constructed a femtosecond laser processing system with a target tracking feature. The block matching method using a sum of squared difference (SSD) metric was used to measure target movement in the transverse direction. The exhaustive search method was stable but required much computing time. In contrast, the steepest descent method was fast method but unstable. The most suitable method should therefore be selected for the application. An astigmatic focus error detection method was used to measure the surface position in the optical axis direction. This system could measure an axial difference from -5.4 µm to 3.8 µm per cycle. The system could track a velocity of 150 µm/s in the transverse direction and 100 µm/s in the optical axis direction. To improve the tracking performance, a faster mechanism for adjusting the focus and a faster block-matching algorithm are required. For example, an algorithm that is three times faster than the exhaustive search in a full-search of SSD has been reported in the field of computer vision [11].

References

[1] E. N. Glezer and E. Mazur: Appl. Phys. Lett., **71** (1997) 882.
[2] H.-B. Sun, T. Tanaka, K. Takada, and S. Kawata: Appl. Phys. Lett., **79** (2001) 1411.
[3] K. Yamasaki, S. Juodkazis, M. Watanabe, H.-B. Sun, S. Matsuo, and H. Misawa: Appl. Phys. Lett., **76** (2000) 1000.
[4] B.-M. Kim, M. D. Feit, A. M. Rubenchik, E. J. Joslin, P. M. Celliers, J. Eichler, and L. B. Da Silva: J. Biomed. Opt., **6** (2001) 332.
[5] A. Takita, M. Watanabe, H. Yamamoto, S. Matsuo, H. Misawa, Y. Hayasaki, and N. Nishida: Jpn. J. Appl. Phys. **43** (2004) 168.
[6] Y. Hayasaki, H. Takagi, A. Takita, H. Yamamoto, N. Nishida, and H. Misawa: Jpn. J. Appl. Phys. **43** (2004) 8089.
[7] A. Takita, H. Yamamoto, Y. Hayasaki, and N. Nishida: Optics Express, **13** (2005) 4560.
[8] D. I. Barnea and H. F. Silverman: IEEE Trans. Comp., **c-21**, (1972) 179.
[9] M. Shimizu and M. Okutomi: Sys. and Com. in Jpn., **36**, 2 (2005) 1.
[10]C. Bricot, J. C. Lahureau, and C. Puech: IEEE Trans. Cons. Electr., **22** (1976) 304.
[11]S. L. Kilthau, M. S. Drew, and T. Möller: Proc. Int. Conf. on Image Proc., New York (2002) I-669.